

# Eigenfrequencies of advanced composite plates using an efficient hybrid quasi-3D shear deformation theory

Hicham Zakaria Guerroudj<sup>1,2</sup>, Redha Yeghnem<sup>\*1,3</sup>, Abdelhakim Kaci<sup>1,3</sup>, Fatima Zohra Zaoui<sup>4</sup>, Samir Benyoucef<sup>3</sup> and Abdelouahed Tounsi<sup>3,5</sup>

<sup>1</sup>University of SAIDA Dr MOULAY TAHAR, Faculty of Technology, Department of Civil Engineering and Hydraulics, PBox 138  
City En-Nasr 20000 SAIDA, Algeria

<sup>2</sup>Laboratory of Ressources Hydriques et Environnement, University Dr MOULAY TAHAR, PBox 138  
City En-Nasr 20000 SAIDA, Algeria

<sup>3</sup>Material and Hydrology Laboratory, University of SIDI BEL ABBES, Algeria

<sup>4</sup>Department of Mechanical Engineering, Faculty of Science and Technology, University of MOSTAGANEM, Algeria

<sup>5</sup>Department of Civil Engineering and Public Works, Faculty of Technology, University of SIDI BEL ABBES, Algeria

(Received January 14, 2018, Revised May 7, 2018, Accepted May 10, 2018)

**Abstract.** This research investigates the free vibration analysis of advanced composite plates such as functionally graded plates (FGPs) resting on a two-parameter elastic foundations using a hybrid quasi-3D (trigonometric as well as polynomial) higher-order shear deformation theory (HSDT). This present theory, which does not require shear correction factor, accounts for shear deformation and thickness stretching effects by a sinusoidal and parabolic variation of all displacements across the thickness. Governing equations of motion for FGM plates are derived from Hamilton's principle. The closed form solutions are obtained by using Navier technique, and natural frequencies are found, for simply supported plates, by solving the results of eigenvalue problems. The accuracy of the present method is verified by comparing the obtained results with First-order shear deformation theory, and other predicted by quasi-3D higher-order shear deformation theories. It can be concluded that the proposed theory is efficient and simple in predicting the natural frequencies of functionally graded plates on elastic foundations.

**Keywords:** free vibration; functionally graded plates; high-order theory; two-parameter elastic foundations; stretching effect

## 1. Introduction

Functionally graded material (FGM) is inhomogeneous composite materials, proposed for the first time in 1984 by materials scientists in the Sendai area (Koizumi 1993, Koizumi 1997) as thermal barrier. FGM is characterized by variation in material properties from one surface to a further along the thickness direction. This concept of FGM can effectively eliminate the interface problems commonly found in composite materials due to stress concentration under the action of external mechanical and/or thermal loads. Those advanced composite materials have the primary constituents made from a mixture of metal with ceramic or from a combination of materials. The FGM is now being used in many structural applications: aircraft, spacecraft (Kar and Panda, 2015a, Xu and Xing 2016), and in other various fields: civil, gas turbines, nuclear fusions, biomaterial electronics, optical thin layers (Bensaid *et al.* 2017) and other engineering and technological applications (Miyamoto *et al.* 1999). This flexibility in design for the FGM is given by their strength and stiffness.

In recent years, a number of studies and computational techniques have been performed and applied for

engineering fields to analyze the static, dynamic and buckling behaviors of FG plates (Jha *et al.* 2013, Kar and Panda 2013, Sobhy 2013, Ait Amar Meziane *et al.* 2014, Kar and Panda 2014, Meksi *et al.* 2015, Attia *et al.* 2015, Kar 2015a, b, Kar and Panda 2015b, c, d, Boudierba *et al.* 2016, Kar and Panda 2016a, b, c, d, Houari *et al.* 2016, Boukhari *et al.* 2016, Kar *et al.* 2017, Kar and Panda 2017a, b, Mahapatra *et al.* 2017, Neves *et al.* 2017) led to the development of various plate theories. However, this behavior can be predicted using either, the classical plate theory (CPT), first-order shear deformation plate theory (FSDT) and higher-order plate theory (HSDT). The classical plate theory (CPT) neglects transverse shear deformation effect (Feldman and Aboudi 1997, Javaheri and Eslami 2002, Chen *et al.* 2006, Abrate 2008, Zhang *et al.* 2008, Mahdavian 2009, Mohammadi *et al.* 2010, Baferani *et al.* 2011) and it is acceptable only for thin plates. The first-order shear deformation plate theory (FSDT) has been used for FG thick and moderately thick plates (Yaghoobi and Yaghoobi 2013, Mantari and Granados 2015, Bellifa *et al.* 2016). This theory takes into account the transverse shear deformation effects and requires an appropriate shear correction factor in order to satisfy the zero transverse shear stress boundary conditions at the top and bottom of the plate. The second-order shear deformation plate theory (SSDT) has been used by Saidi and Sahraee (2006). They studied axisymmetric bending and stretching of functionally graded

\*Corresponding author, Ph.D.

E-mail: yeghnemreda2000@yahoo.fr

solid circular and annular plates. Khdeir and Reddy (1999) studied the free vibration of laminated composite plates using SSDT. Shahrjerdi and Mustapha (2011) have been used SSDT to study the free vibration of FG plates (rectangular and square). Karami et al. (2018) used SSDT to study wave dispersion of mounted graphene with initial stress. Nami et al. (2015) were used nonlocal third-order shear deformation theory to analyze the thermal buckling of FG rectangular nanoplates. Alternatively, several higher-order shear deformation plate theories (HSDT) have been proposed for FG plates, with higher-order variations of displacements (Neves et al. 2012, Bouazza et al. 2015, Bensatallah et al. 2016). A large number of studies have been performed to study the mechanical behavior of advanced composite plates using non-polynomial functions (hyperbolic, sinusoidal, exponential and tangent). The aim to use these functions is to describe the warping through the thickness, taking into account the transverse shear deformation effect in the plate. Mantari et al. (2012) employed the non-polynomial trigonometric function in the displacement to study the bending response of sandwich and laminated plates. Also, Mantari (2015) studied the bending analysis of functionally graded shells by presenting a closed-form solution of a generalized hybrid type quasi-3D higher order shear deformation theory. The buckling behavior of sandwich plates with functionally graded skins using a new quasi-3D hyperbolic sine shear deformation theory has been studied by Neves et al. (2012). Tounsi and his co-workers (Ait Amar Meziane et al. 2014, Attia et al. 2015, Hassaine Daouadji et al. 2015 and Bousahla et al. 2016) developed a new refined plate theory for free vibration analysis of functionally graded materials with four unknown functions. They introduced undetermined integral variables into the displacement field. This theory does not require shear correction factor and satisfies the zero transverse shear on the surfaces of the plate. The thickness stretching effect is ignored in the above theory and the transverse displacement is considered constant in the thickness direction, as in Kirchhoff-Love type thin FGM plates. The majority of higher-order shear deformation theories employed to investigate the mechanical behavior of FGM plates contain five unknowns. In order to diminish the number of variables used in the equilibrium equation, satisfying the shear deformation effects on the bottom and top surfaces of plate without employing shear correction factor, many refined theories have been offered. Shimpi and Patel (2006) have studied the free vibration of plate using two variable refined plate theory. Nguyen et al. (2015) have studied the bending, vibration and buckling analysis of FG sandwich plates using a refined shear deformation theory. Karami et al. (2017) were used a four variable refined plate theory to study the wave propagation analysis in FG nanoplates under in-plane magnetic field based on nonlocal strain gradient theory. Karami and Janghorban (2016) have been used one parameter and two-variable refined plate theory to study the effect of magnetic field on the wave propagation in nanoplates based on strain gradient theory. Always, Karami and Janghorban (2018) were studied wave propagation in fully clamped porous FG nanoplates.

From the literature, there have been many studies on the

bending, vibration and buckling behaviors of FGM plates resting on elastic foundations (Ait Atmane et al. 2010, Abualnour et al. 2018, Shahsavari et al. 2018, Ait Atmane and Tounsi 2017). Meftah et al. (2017) studied the free vibration of FG thick rectangular plates on elastic foundation using a non-polynomial four variable refined plate theory. Shahsavari et al. (2018) have studied the shear buckling of single layer graphene sheets in hygrothermal environment resting on elastic foundation based on different nonlocal strain gradient theories. These foundations considered include the Winkler and Pasternak type elastic foundations.

In this paper, the vibration analysis of FGMs plates is analyzed based on a simple and efficient hybrid quasi-3D higher-order shear deformation plate theory. The highlight of this theory is that, in addition to including the Winkler-Pasternak elastic foundations and the thickness stretching effect, the displacement field contains only five unknowns against six or more displacement functions used in other theories. Governing equations of motion for FGM plates are derived from Hamilton's principle. The closed form solutions are obtained by using Navier technique, and natural frequencies are found, for simply supported plates, by solving the results of eigenvalue problems. Moreover, the accuracy of the hybrid quasi-3D HSDT is examined by comparing the present results with published ones.

The paper is organized as following. Section 2 outlines the geometric configuration and material properties of FGMs plates. Section 3 describes the theoretical formulation methodology of FGMs, constitutive relations, displacement field and strains, plate governing equations, equations of motion in terms of displacements and analytical solutions. The last section 4 is about numerical results and discussions. Finally, further general aspects are given in the conclusions.

## 2. Geometric configuration and material properties

Consider an FG plate of length  $a$ , width  $b$ , and thickness  $h$  that is made of a FGM and resting on elastic foundation (Fig. 1). The FGM is assumed to vary from the ceramic-rich top surface ( $z = h/2$ ) to the metal-rich bottom surface ( $z = -h/2$ ). The rectangular Cartesian coordinate system  $x, y, z$  has the plane  $z = 0$ .

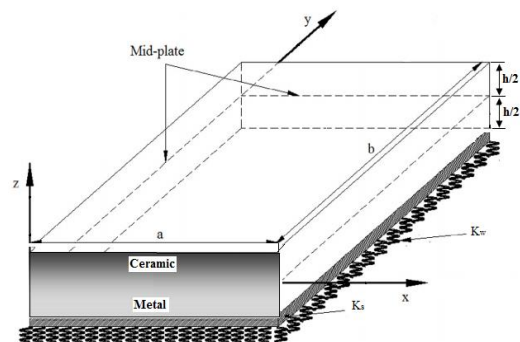


Fig. 1 Geometry of FGM plate resting on Winkler-Pasternak foundation

The effective Young's modulus  $E$  of the FGM plate can be expressed in a power law as (Reddy2000)

$$P(z) = P_m + (P_c - P_m) \left( \frac{1}{2} + \frac{z}{h} \right)^p \quad (1)$$

In which the variables with subscripts c and m denote the properties of the top and bottom surfaces of the plate, respectively, and  $p$  is the power law index. The volume fraction index  $p$  specifies the material variation profile through the thickness. The value  $p = 0$  represents a ceramic plate.

### 3. Theoretical formulation

#### 3.1 Constitutive relations

The linear constitutive relations of the FG plates are written as

$$\begin{Bmatrix} \sigma_x \\ \sigma_y \\ \sigma_z \\ \tau_{yz} \\ \tau_{xz} \\ \tau_{xy} \end{Bmatrix} = \begin{bmatrix} Q_{11} & Q_{12} & Q_{13} & 0 & 0 & 0 \\ Q_{12} & Q_{22} & Q_{23} & 0 & 0 & 0 \\ Q_{13} & Q_{23} & Q_{33} & 0 & 0 & 0 \\ 0 & 0 & 0 & Q_{44} & 0 & 0 \\ 0 & 0 & 0 & 0 & Q_{55} & 0 \\ 0 & 0 & 0 & 0 & 0 & Q_{66} \end{bmatrix} \begin{Bmatrix} \varepsilon_x \\ \varepsilon_y \\ \varepsilon_z \\ \gamma_{yz} \\ \gamma_{xz} \\ \gamma_{xy} \end{Bmatrix} \quad (2)$$

Where  $(\sigma_x, \sigma_y, \sigma_z, \tau_{yz}, \tau_{xz}, \tau_{xy})$  and  $(\varepsilon_x, \varepsilon_y, \varepsilon_z, \gamma_{yz}, \gamma_{xz}, \gamma_{xy})$  are the stress and the strain components, respectively. The stiffness coefficients  $Q_{ij}$  are given by

$$Q_{11} = Q_{22} = Q_{33} = \frac{E(z)(1-\nu)}{(1-2\nu)(1+\nu)} \quad (3a)$$

$$Q_{12} = Q_{13} = Q_{23} = \frac{\nu E(z)}{(1-2\nu)(1+\nu)} \quad (3b)$$

$$Q_{44} = Q_{55} = Q_{66} = \frac{E(z)}{2(1+\nu)} \quad (3c)$$

#### 3.2 Displacement field and strains

Basic assumptions for the displacement field of the plate, including the transverse normal stress effect are given as (Mahi *et al.* 2015)

$$u(x, y, z, t) = u_0(x, y, t) - z \frac{\partial w_b}{\partial x} + f(z) \frac{\partial w_s}{\partial x}(x, y, t) \quad (4a)$$

$$v(x, y, z, t) = v_0(x, y, t) - z \frac{\partial w_b}{\partial y} + f(z) \frac{\partial w_s}{\partial y}(x, y, t) \quad (4b)$$

$$w(x, y, z, t) = w_b(x, y, t) + g(z) \varphi_z(x, y, t) \quad (4c)$$

Where  $u_0$  and  $v_0$  are the in-plane displacements of the geometrical mid-plane of the plate along the  $x$  and  $y$  directions.  $w_b$  and  $w_s$  are the bending and shear components of the transverse displacement, respectively, and the additional displacement  $\varphi_z$  accounts for the effect of normal stress.  $f(z)$  and  $g(z)$  represent shape functions defining the distribution of the transverse shear strains and stress through the thickness.

Based on the thick plate theory and including the thickness stretching effect (effect of transverse normal stress), the basic assumptions for the displacement field of the FG plate can be expressed as follows (Abualnour *et al.* 2018)

$$u(x, y, z, t) = u_0(x, y, t) - z \frac{\partial w_b}{\partial x} + k_1 f(z) \int \theta(x, y, t) dx \quad (5a)$$

$$v(x, y, z, t) = v_0(x, y, t) - z \frac{\partial w_b}{\partial y} + k_2 f(z) \int \theta(x, y, t) dy \quad (5b)$$

$$w(x, y, z, t) = w_0(x, y, t) + g(z) \varphi_z(x, y, t) \quad (5c)$$

The coefficients  $k_1$  and  $k_2$  depend on the geometry of the FG plate. The displacements field of the present theory, satisfying the conditions of transverse shear stresses (and hence strains) on the top and bottom surfaces of the plate, is given in simpler form as

$$u(x, y, z, t) = u_0(x, y, t) - z \frac{\partial w_b}{\partial x} + k_1 A' f(z) \frac{d\theta}{dx} \quad (6a)$$

$$v(x, y, z, t) = v_0(x, y, t) - z \frac{\partial w_b}{\partial y} + k_2 \beta' f(z) \frac{d\theta}{dy} \quad (6b)$$

$$w(x, y, z, t) = w_b(x, y, t) + g(z) \varphi(x, y, t) \quad (6c)$$

It is clearly seen that the displacement field in Eq. (6) handles only five unknowns, i.e.,  $u_0, v_0, w_b, \theta$  and  $\varphi$ .

In this study, the shape functions  $f(z)$  and  $g(z)$  are chosen based on the trigonometric form (Mahi *et al.* 2015)

$$f(z) = \frac{h}{2} \tanh \frac{2z}{h} - \frac{4}{3} \frac{z^3}{h^2 \cosh(l)^2} \quad (7)$$

$$g(z) = 1 - 4 \left( \frac{z}{h} \right)^2 \quad (8)$$

The non-zero strains associated with the new displacement field in Eq. (6) are

$$\begin{Bmatrix} \varepsilon_x \\ \varepsilon_y \\ \gamma_{xy} \end{Bmatrix} = \begin{Bmatrix} \varepsilon_x^0 \\ \varepsilon_y^0 \\ \gamma_{xy}^0 \end{Bmatrix} + z \begin{Bmatrix} k_x^b \\ k_y^b \\ k_{xy}^b \end{Bmatrix} + f(z) \begin{Bmatrix} k_x^s \\ k_y^s \\ k_{xy}^s \end{Bmatrix} \quad (9a)$$

$$\begin{Bmatrix} \gamma_{yz} \\ \gamma_{xz} \end{Bmatrix} = f'(z) \begin{Bmatrix} \gamma_{yz}^0 \\ \gamma_{xz}^0 \end{Bmatrix} + g(z) \begin{Bmatrix} \gamma_{yz}^1 \\ \gamma_{xz}^1 \end{Bmatrix} \quad (9b)$$

$$\varepsilon_z = g'(z) \varepsilon_z^0 \quad (9c)$$

where

$$\begin{Bmatrix} \varepsilon_x^0 \\ \varepsilon_y^0 \\ \gamma_{xy}^0 \end{Bmatrix} = \begin{Bmatrix} \frac{\partial u_0}{\partial x} \\ \frac{\partial v_0}{\partial y} \\ \frac{\partial u_0}{\partial y} + \frac{\partial v_0}{\partial x} \end{Bmatrix} \quad (10a)$$

$$\begin{Bmatrix} k_x^b \\ k_y^b \\ k_{xy}^b \end{Bmatrix} = \begin{Bmatrix} -\frac{\partial^2 w_b}{\partial x^2} \\ -\frac{\partial^2 w_b}{\partial y^2} \\ -2\frac{\partial^2 w_b}{\partial x \partial y} \end{Bmatrix} \quad (10b)$$

$$\begin{Bmatrix} k_x^s \\ k_y^s \\ k_{xy}^s \end{Bmatrix} = \begin{Bmatrix} k_1 A' \frac{\partial^2 \theta}{\partial x^2} \\ k_2 B' \frac{\partial^2 \theta}{\partial y^2} \\ (k_1 A' + k_2 B') \frac{\partial^2 \theta}{\partial x \partial y} \end{Bmatrix} \quad (10c)$$

$$\begin{Bmatrix} \gamma_{yz}^0 \\ \gamma_{xz}^0 \end{Bmatrix} = \begin{Bmatrix} k_2 B' \frac{\partial \theta}{\partial y} \\ k_1 A' \frac{\partial \theta}{\partial x} \end{Bmatrix} \quad (10d)$$

$$\begin{Bmatrix} \gamma_{yz}^1 \\ \gamma_{xz}^1 \end{Bmatrix} = \begin{Bmatrix} \frac{\partial \varphi_z}{\partial y} \\ \frac{\partial \varphi_z}{\partial x} \end{Bmatrix} \quad (10e)$$

$$\varepsilon_z^0 = \varphi_z, \quad g'(z) = \frac{\partial g(z)}{\partial z} \quad (10f)$$

It can be seen from Eq. (9) that the transverse shear strains ( $\gamma_{yz}$  and  $\gamma_{xz}$ ) are equal to zero at the top ( $z = h/2$ ) and the bottom ( $z = -h/2$ ) surfaces of the FG plate.

We used the Navier type procedure to resolve integrals used in the above equations. We can express them as

$$\frac{\partial}{\partial y} \int \theta dx = A' \frac{\partial^2 \theta}{\partial x \partial y}, \quad \frac{\partial}{\partial x} \int \theta dy = B' \frac{\partial^2 \theta}{\partial x \partial y}, \quad (11)$$

$$\int \theta dx = A' \frac{\partial \theta}{\partial x}, \quad \int \theta dy = B' \frac{\partial \theta}{\partial y}$$

The coefficients  $A'$  and  $B'$  are depending on the solution type obtained by Navier method. We give below  $A'$ ,  $B'$ ,  $k_1$  and  $k_2$

$$A' = -\frac{1}{\alpha^2}, \quad B' = -\frac{1}{\beta^2}, \quad k_1 = \alpha^2, \quad k_2 = \beta^2 \quad (12)$$

$\alpha$  and  $\beta$  are defined in Eq. (27).

### 3.3 Plate governing equations

Hamilton's principle is employed to derive the equations of motion. It can be stated as (Reddy 2002, Bennoun et al. 2016)

$$0 = \int_0^t (\delta U + \delta V_e - \delta K) dt \quad (13)$$

The variation of strain energy is expressed as

$$\begin{aligned} \delta U = & \int_V [\sigma_x \delta \varepsilon_x + \sigma_y \delta \varepsilon_y + \sigma_z \delta \varepsilon_z + \tau_{xy} \delta \gamma_{xy} + \tau_{yz} \delta \gamma_{yz} + \tau_{xz} \delta \gamma_{xz}] dAdV \\ = & \int_A \left[ N_x \delta \varepsilon_x^0 + N_y \delta \varepsilon_y^0 + N_z \delta \varepsilon_z^0 + N_{xy} \delta \gamma_{xy}^0 + M_x^b \delta k_x^b + M_y^b \delta k_y^b + \right. \\ & \left. M_{xy}^b \delta k_{xy}^b + M_x^s \delta k_x^s + M_y^s \delta k_y^s + M_{xy}^s \delta k_{xy}^s + Q_{yz}^s \delta \gamma_{yz}^0 + S_{yz}^s \delta \gamma_{yz}^1 + Q_{xz}^s \delta \gamma_{xz}^0 \right. \\ & \left. + S_{xz}^s \delta \gamma_{xz}^1 \right] dA \end{aligned} \quad (14)$$

where  $A$  is the top surface and stress resultants  $N, M, S$  and  $Q$  are given by

$$\begin{aligned} (N_i, M_i^b, M_i^s) &= \int_{-h/2}^{h/2} (1, z, f) \sigma_i dz, \quad (i = x, y, xy), \\ N_z &= \int_{-h/2}^{h/2} g'(z) \sigma_z dz \end{aligned} \quad (15)$$

and

$$\begin{aligned} (S_{xz}^s, S_{yz}^s) &= \int_{-h/2}^{h/2} g(\tau_{xz}, \tau_{yz}) dz, \\ (Q_{xz}^s, Q_{yz}^s) &= \int_{-h/2}^{h/2} f'(\tau_{xz}, \tau_{yz}) dz \end{aligned} \quad (16)$$

$$\delta V_e = \int_A f_e \delta w_0 dA \quad (17)$$

$$f_e = K_w w - K_s \left( \frac{\partial^2 w}{\partial x^2} + \frac{\partial^2 w}{\partial y^2} \right) \quad (18)$$

The plate kinetic energy is expressed by

$$\begin{aligned} \delta K = & \int_V [\dot{u} \delta \dot{u} + \dot{v} \delta \dot{v} + \dot{w} \delta \dot{w}] \rho(z) dV \\ = & \int_A \left[ I_0 (\dot{u}_0 \delta \dot{u}_0 + \dot{v}_0 \delta \dot{v}_0 + \dot{w}_0 \delta \dot{w}_0) + J_0 (\dot{w}_0 \delta \dot{\phi}_z + \dot{\phi}_z \delta \dot{w}_0) \right. \\ & - I_1 \left( \dot{u}_0 \frac{\partial \delta \dot{w}_0}{\partial x} + \frac{\partial \dot{w}_0}{\partial x} \delta \dot{u}_0 + \dot{v}_0 \frac{\partial \delta \dot{w}_0}{\partial y} + \frac{\partial \dot{w}_0}{\partial y} \delta \dot{v}_0 \right) \\ & + J_1 \left( k_1 A' \left( \dot{u}_0 \frac{\partial \delta \dot{\theta}}{\partial x} + \frac{\partial \dot{\theta}}{\partial x} \delta \dot{u}_0 \right) + k_2 B' \left( \dot{v}_0 \frac{\partial \delta \dot{\theta}}{\partial y} + \frac{\partial \dot{\theta}}{\partial y} \delta \dot{v}_0 \right) \right) \\ & + I_2 \left( \frac{\partial \dot{w}_0}{\partial x} \frac{\partial \delta \dot{w}_0}{\partial x} + \frac{\partial \dot{w}_0}{\partial y} \frac{\partial \delta \dot{w}_0}{\partial y} \right) + K_2 \left( (k_1 A')^2 \frac{\partial \dot{\theta}}{\partial x} \frac{\partial \delta \dot{\theta}}{\partial x} + (k_2 B')^2 \frac{\partial \dot{\theta}}{\partial y} \frac{\partial \delta \dot{\theta}}{\partial y} \right) \\ & \left. - J_2 \left( k_1 A' \left( \frac{\partial \dot{w}_0}{\partial x} \frac{\partial \delta \dot{\theta}}{\partial x} + \frac{\partial \dot{\theta}}{\partial x} \frac{\partial \delta \dot{w}_0}{\partial x} \right) + k_2 B' \left( \frac{\partial \dot{w}_0}{\partial y} \frac{\partial \delta \dot{\theta}}{\partial y} + \frac{\partial \dot{\theta}}{\partial y} \frac{\partial \delta \dot{w}_0}{\partial y} \right) \right) + K_0 \dot{\phi}_z \delta \dot{\phi}_z \right] dA \end{aligned} \quad (19)$$

where  $(I_0, I_1, I_2, J_1, J_2, J_0, K_0, K_2)$  are mass inertias given below by formulas (20a) and (20b).  $\rho(z)$  is the mass density.

$$(I_0, I_1, I_2, J_1) = \int_{-h/2}^{h/2} (1, z, z^2, f(z)) \rho(z) dz \quad (20a)$$

$$(J_2, J_0, K_0, K_2) = \int_{-h/2}^{h/2} (zf'(z), g(z), g^2(z), f^2(z)) \rho(z) dz \quad (20b)$$

Substituting the expressions for  $\delta U$ ,  $\delta V_e$  and  $\delta K$  from Eqs. (14), (17) and (19) into Eq. (13) and integrating by parts and collecting the coefficients of  $\delta u_0$ ,  $\delta v_0$ ,  $\delta w_0$ ,  $\delta \theta$  and  $\delta \phi_z$ , the equations of motion of the plate are expressed by

$$\begin{aligned} \delta u_0 : & \frac{\partial N_x}{\partial x} + \frac{\partial N_{xy}}{\partial y} = I_0 \ddot{u}_0 - I_1 \frac{\partial \ddot{w}_0}{\partial x} + J_1 k_1 A' \frac{\partial \ddot{\theta}}{\partial x} \\ \delta v_0 : & \frac{\partial N_y}{\partial y} + \frac{\partial N_{xy}}{\partial x} = I_0 \ddot{v}_0 - I_1 \frac{\partial \ddot{w}_0}{\partial y} + J_1 k_2 B' \frac{\partial \ddot{\theta}}{\partial y} \\ \delta w_0 : & \frac{\partial^2 M_x^b}{\partial x^2} + \frac{\partial^2 M_y^b}{\partial y^2} + 2 \frac{\partial^2 M_{xy}^b}{\partial x \partial y} - f_e = I_0 \ddot{w}_0 + J_0 \ddot{\phi} + \\ & I_1 \left( \frac{\partial \ddot{u}_0}{\partial x} + \frac{\partial \ddot{v}_0}{\partial y} \right) - I_2 \nabla \ddot{w}_0 + J_2 (k_1 A' \frac{\partial^2 \ddot{\theta}}{\partial x^2} + k_2 B' \frac{\partial^2 \ddot{\theta}}{\partial y^2}) \\ \delta \theta : & -k_1 M_x^s - k_2 M_y^s - (k_1 A' + k_2 B') \frac{\partial^2 M_{xy}^s}{\partial x \partial y} + \\ & k_1 A' \frac{\partial Q_{xz}^s}{\partial x} + k_2 B' \frac{\partial Q_{yz}^s}{\partial y} = -J_1 (k_1 A' \frac{\partial \ddot{u}_0}{\partial x} + k_2 B' \frac{\partial \ddot{v}_0}{\partial y}) \\ & + J_2 (k_1 A' \frac{\partial^2 \ddot{w}_0}{\partial x^2} + k_2 B' \frac{\partial^2 \ddot{w}_0}{\partial y^2}) - K_2 ((k_1 A')^2 \frac{\partial^2 \ddot{\theta}}{\partial x^2} + (k_2 B')^2 \frac{\partial^2 \ddot{\theta}}{\partial y^2}) \\ \delta \phi_z : & \frac{\partial S_{xz}^s}{\partial x} + \frac{\partial S_{yz}^s}{\partial y} - N_z = J_0 \ddot{w}_0 + K_0 \ddot{\phi}_z \end{aligned} \quad (21)$$

Using Eqs. (6) in (20), the stress resultant of FG plate is related to the total strain by

$$\begin{Bmatrix} N_x \\ N_y \\ N_{xy} \\ M_x^b \\ M_y^b \\ M_{xy}^b \\ M_x^s \\ M_y^s \\ M_{xy}^s \\ N_z \end{Bmatrix} = \begin{Bmatrix} A_{11} & A_{12} & 0 & B_{11} & B_{12} & 0 & B_{11}^s & B_{12}^s & 0 & X_{13} \\ A_{12} & A_{22} & 0 & B_{12} & B_{22} & 0 & B_{12}^s & B_{22}^s & 0 & X_{23} \\ 0 & 0 & A_{66} & 0 & 0 & 0 & B_{66}^s & 0 & 0 & B_{66}^s \\ B_{11} & B_{12} & 0 & D_{11} & D_{12} & 0 & D_{11}^s & D_{12}^s & 0 & Y_{13} \\ B_{12} & B_{22} & 0 & D_{12} & D_{22} & 0 & D_{12}^s & D_{22}^s & 0 & Y_{23} \\ 0 & 0 & B_{66} & 0 & 0 & D_{11} & 0 & 0 & D_{66}^s & 0 \\ B_{11}^s & B_{12}^s & 0 & D_{11}^s & D_{12}^s & 0 & H_{11}^s & H_{12}^s & 0 & Y_{13}^s \\ B_{12}^s & B_{22}^s & 0 & D_{12}^s & D_{22}^s & 0 & H_{12}^s & H_{22}^s & 0 & Y_{23}^s \\ 0 & 0 & B_{66}^s & 0 & 0 & D_{66}^s & 0 & 0 & H_{66}^s & 0 \\ X_{13} & X_{23} & 0 & Y_{13} & Y_{23} & 0 & Y_{13}^s & Y_{23}^s & 0 & Z_{33} \end{Bmatrix} \begin{Bmatrix} \frac{\partial u_0}{\partial x} \\ \frac{\partial v_0}{\partial y} \\ \frac{\partial u_0}{\partial y} + \frac{\partial v_0}{\partial x} \\ -\frac{\partial^2 w_0}{\partial x^2} \\ -\frac{\partial^2 w_0}{\partial y^2} \\ -2 \frac{\partial^2 w_0}{\partial x \partial y} \\ k_1 \theta \\ k_2 \theta \\ (k_1 A' + k_2 B') \frac{\partial^2 \theta}{\partial x \partial y} \\ \phi_z \end{Bmatrix} \quad (22a)$$

$$\begin{Bmatrix} S_{yz}^s \\ S_{xz}^s \end{Bmatrix} = \begin{Bmatrix} G_{44}^s & A_{44}^s \\ G_{55}^s & A_{55}^s \end{Bmatrix} \begin{Bmatrix} k_2 B' \frac{\partial \theta}{\partial y} & k_1 A' \frac{\partial \theta}{\partial x} \\ \frac{\partial \phi_z}{\partial y} & \frac{\partial \phi_z}{\partial x} \end{Bmatrix} \quad (22b)$$

$$\begin{Bmatrix} Q_{yz}^s \\ Q_{xz}^s \end{Bmatrix} = \begin{Bmatrix} F_{44}^s & G_{44}^s \\ F_{55}^s & G_{55}^s \end{Bmatrix} \begin{Bmatrix} k_2 B' \frac{\partial \theta}{\partial y} & k_1 A' \frac{\partial \theta}{\partial x} \\ \frac{\partial \phi_z}{\partial y} & \frac{\partial \phi_z}{\partial x} \end{Bmatrix} \quad (22c)$$

where

$$(A_{ij}, A_{ij}^s, B_{ij}) = \int_{-h/2}^{h/2} Q_{ij} (1, g^2(z), z) dz \quad (23a)$$

$$(D_{ij}, B_{ij}^s, D_{ij}^s) = \int_{-h/2}^{h/2} Q_{ij} (z^2, f(z), z f(z)) dz \quad (23b)$$

$$(H_{ij}^s, F_{ij}^s, G_{ij}^s) = \int_{-h/2}^{h/2} Q_{ij} (f^2(z), f'^2(z), f'(z)g(z)) dz \quad (23c)$$

$$(X_{ij}, Y_{ij}, Y_{ij}^s, Z_{ij}) = \int_{-h/2}^{h/2} Q_{ij} (1, z, f(z), g'(z)) g'(z) dz \quad (23d)$$

### 3.4 Equations of motion in terms of displacements

Introducing Eq. (22) into Eq. (21), the equilibrium equations can be expressed in terms of displacements  $u_0$ ,  $v_0$ ,  $w_0$ ,  $\theta$  and  $\phi_z$  by following formulas.

$$\begin{aligned}
& A_{11} d_{11} u_0 + A_{66} d_{22} u_0 + (A_{12} + A_{66}) d_{12} v_0 \\
& - B_{11} d_{111} w_0 - (B_{12} + 2B_{66}) d_{122} w_0 + \\
& (k_1 B_{11}^s + k_2 B_{12}^s) d_1 \theta + (k_1 A' + k_2 B') B_{66}^s d_{122} \theta + X_{13} d_1 \varphi_z \quad (24a) \\
& = I_0 \ddot{u}_0 - I_1 d_1 \ddot{w}_0 + (k_1 A') J_1 d_1 \ddot{\theta}
\end{aligned}$$

$$\begin{aligned}
& (A_{12} + A_{66}) d_{12} u_0 + A_{66} d_{11} v_0 + A_{22} d_{22} v_0 \\
& - (B_{12} + 2B_{66}) d_{112} w_0 - B_{22} d_{222} w_0 + \\
& (k_1 B_{12}^s + k_2 B_{22}^s) d_2 \theta + (k_1 A' + k_2 B') B_{66}^s d_{112} \theta + X_{23} d_2 \varphi_z \quad (24b) \\
& = I_0 \ddot{v}_0 - I_1 d_2 \ddot{w}_0 + J_1 k_2 B' d_2 \ddot{\theta}
\end{aligned}$$

$$\begin{aligned}
& B_{11} d_{111} u_0 + (B_{12} + 2B_{66}) d_{122} u_0 + (B_{12} + 2B_{66}) d_{112} v_0 \\
& + B_{22} d_{222} v_0 - D_{11} d_{1111} w_0 - D_{22} d_{2222} w_0 \\
& - 2(D_{12} + 2D_{66}) d_{1122} w_0 + (k_1 D_{11}^s + k_2 D_{12}^s) d_{11} \theta \\
& + (k_1 D_{12}^s + k_2 D_{22}^s) d_{22} \theta + 2(k_1 A' + k_2 B') D_{66}^s d_{1122} \theta \quad (24c) \\
& + Y_{13} d_{11} \varphi_z + Y_{23} d_{22} \varphi_z - f_e = I_0 \ddot{w}_0 + J_0 \ddot{\varphi}_z \\
& + I_1 (d_1 \ddot{u}_0 + d_2 \ddot{v}_0) - I_2 \nabla^2 \ddot{w}_0 + J_2 (k_1 A' d_{11} \ddot{\theta} + k_2 B' d_{22} \ddot{\theta})
\end{aligned}$$

$$\begin{aligned}
& - (k_1 B_{11}^s + k_2 B_{12}^s) d_1 u_0 - (k_1 B_{12}^s + k_2 B_{22}^s) d_2 v_0 \\
& - B_{66}^s (k_1 A' + k_2 B') (d_{122} u_0 + d_{112} v_0) \\
& + (k_1 D_{11}^s + k_2 D_{12}^s) d_{11} w_0 + (k_1 D_{12}^s + k_2 D_{22}^s) d_{22} w_0 \\
& + 2D_{66}^s (k_1 A' + k_2 B') d_{1122} w_0 \\
& - (k_1^2 H_{11}^s + k_2^2 H_{22}^s + 2k_1 k_2 H_{12}^s) \theta + (k_1 A')^2 F_{55}^s d_{11} \theta \\
& + (k_2 B')^2 F_{44}^s d_{22} \theta - H_{66}^s (k_1 A' + k_2 B')^2 d_{1122} \theta \quad (24d) \\
& - (k_1 Y_{13}^s + k_2 Y_{23}^s) \varphi_z + k_1 A' G_{55}^s d_{11} \varphi_z \\
& + k_2 B' G_{44}^s d_{22} \varphi_z = -J_1 (k_1 A' d_1 \ddot{u}_0 + k_2 B' d_2 \ddot{v}_0) \\
& + J_2 (k_1 A' d_{11} \ddot{w}_0 + k_2 B' d_{22} \ddot{w}_0) \\
& - K_2 ((k_1 A')^2 d_{11} \ddot{\theta} + (k_2 B')^2 d_{22} \ddot{\theta})
\end{aligned}$$

$$\begin{aligned}
& -X_{13} d_1 u_0 - X_{23} d_2 v_0 + Y_{13} d_{11} w_0 + Y_{23} d_{22} w_0 \\
& + (k_1 (G_{55}^s - Y_{13}^s) + k_2 (G_{44}^s - Y_{23}^s)) \theta + A_{55}^s d_{11} \varphi_z \quad (24e) \\
& + A_{44}^s d_{22} \varphi_z - Z_{33} \varphi_z = J_0 \ddot{w}_0 + K_0 \ddot{\varphi}_z
\end{aligned}$$

where  $d_{ij}$ ,  $d_{ijl}$ ,  $d_{ijlm}$  and  $d_i$  are given by

$$\begin{aligned}
d_{ij} &= \frac{\partial^2}{\partial x_i \partial x_j}, \quad d_{ijl} = \frac{\partial^3}{\partial x_i \partial x_j \partial x_l}, \\
d_{ijlm} &= \frac{\partial^4}{\partial x_i \partial x_j \partial x_l \partial x_m}, \quad d_i = \frac{\partial}{\partial x_i}, \quad (i, j, l, m = 1, 2). \quad (25)
\end{aligned}$$

### 3.5 Analytical solutions

A simply supported rectangular FGM plate is considered with length  $a$  and width  $b$  under transverse load  $q$ . Using

Navier's solution method, the expressions of displacements ( $u_0$ ,  $v_0$ ,  $w_0$ ,  $\theta$  and  $\varphi_z$ ) are given by

$$\begin{Bmatrix} u_0 \\ v_0 \\ w_0 \\ \theta \\ \varphi_z \end{Bmatrix} = \sum_{m=1}^{\infty} \sum_{n=1}^{\infty} \begin{Bmatrix} U_{mn} \cos(\alpha x) \sin(\beta y) e^{i\omega t} \\ V_{mn} \sin(\alpha x) \cos(\beta y) e^{i\omega t} \\ W_{mn} \sin(\alpha x) \sin(\beta y) e^{i\omega t} \\ X_{mn} \sin(\alpha x) \sin(\beta y) e^{i\omega t} \\ \Phi_{mn} \sin(\alpha x) \sin(\beta y) e^{i\omega t} \end{Bmatrix} \quad (26)$$

where  $U_{mn}$ ,  $V_{mn}$ ,  $W_{mn}$ ,  $X_{mn}$  and  $\Phi_{mn}$  unknown displacement coefficients must be determined,  $\omega$  is the Eigen frequency associated with  $(m, n)$  Eigen mode.  $\alpha$  and  $\beta$  are expressed as

$$\alpha = m\pi / a, \quad \beta = n\pi / b \quad (27)$$

Substituting Eq. (26) into Eq. (24), the analytical solutions can be then defined by

$$\begin{pmatrix} \begin{bmatrix} s_{11} & s_{12} & s_{13} & s_{14} & s_{15} \\ s_{12} & s_{22} & s_{23} & s_{24} & s_{25} \\ s_{13} & s_{23} & s_{33} & s_{34} & s_{35} \\ s_{14} & s_{24} & s_{34} & s_{44} & s_{45} \\ s_{15} & s_{25} & s_{35} & s_{45} & s_{55} \end{bmatrix} - \omega^2 \begin{bmatrix} m_{11} & m_{12} & m_{13} & m_{14} & m_{15} \\ m_{12} & m_{22} & m_{23} & m_{24} & m_{25} \\ m_{13} & m_{23} & m_{33} & m_{34} & m_{35} \\ m_{14} & m_{24} & m_{34} & m_{44} & m_{45} \\ m_{15} & m_{25} & m_{35} & m_{45} & m_{55} \end{bmatrix} \end{pmatrix} \begin{Bmatrix} U_{mn} \\ V_{mn} \\ W_{mn} \\ X_{mn} \\ \Phi_{mn} \end{Bmatrix} = \begin{Bmatrix} 0 \\ 0 \\ 0 \\ 0 \\ 0 \end{Bmatrix} \quad (28)$$

where elements of  $s_{ij}$  and  $m_{ij}$  are stiffness and mass matrices respectively. These elements are given by

$$\begin{aligned}
s_{11} &= \alpha^2 A_{11} + \beta^2 A_{66}, \quad s_{12} = \alpha\beta(A_{12} + A_{66}), \\
s_{13} &= -\alpha^3 B_{11} - \alpha\beta^2(B_{12} + 2B_{66}), \\
s_{14} &= -\alpha(k_1 B_{11}^s + k_2 B_{12}^s) + \alpha\beta^2 B_{66}^s (k_1 A' + k_2 B'), \\
s_{15} &= \alpha X_{13}, \quad s_{22} = \alpha^2 A_{66} + \beta^2 A_{22}, \\
s_{23} &= -\alpha^2 \beta(B_{12} + 2B_{66}) - \beta^3 B_{22}, \quad (29) \\
s_{24} &= -\beta(k_1 B_{12}^s + k_2 B_{22}^s) + \alpha^2 \beta(k_1 A' + k_2 B') B_{66}^s, \\
s_{25} &= -\beta X_{23}, \\
s_{33} &= \alpha^4 D_{11} + \beta^4 D_{22} + 2\alpha^2 \beta^2 (D_{12} + 2D_{66}) + \\
& K_w + K_s (\alpha^2 + \beta^2),
\end{aligned}$$

$$s_{34} = \alpha^2 k_1 D_{11}^s + (k_2 \alpha^2 + k_1 \beta^2) D_{12}^s + \beta^2 k_2 D_{22}^s - 2\alpha^2 \beta^2 (k_1 A' + k_2 B') D_{66}^s,$$

$$s_{35} = \alpha^2 Y_{13} + \beta^2 Y_{23},$$

$$s_{44} = k_1^2 H_{11}^s + k_2^2 H_{22}^s + 2k_1 k_2 H_{12}^s + \alpha^2 \beta^2 (k_1 A' + k_2 B')^2 H_{66}^s + \alpha^2 (k_1 A')^2 F_{55}^s + \beta^2 (k_2 B')^2 F_{44}^s,$$

$$s_{45} = k_1 Y_{13}^s + k_2 Y_{23}^s + \alpha^2 k_1 A' G_{55}^s + \beta^2 k_2 B' G_{44}^s,$$

$$s_{55} = \alpha^2 A_{55}^s + \beta^2 A_{44}^s + Z_{33},$$

$$m_{11} = m_{22} = I_0, \quad m_{12} = m_{15} = m_{25} = m_{45} = 0,$$

$$m_{13} = -\alpha I_1, \quad m_{14} = \alpha k_1 A' J_1, \quad m_{15} = 0,$$

$$m_{23} = -\beta I_1,$$

$$m_{24} = \beta k_2 B' J_1, \quad m_{33} = I_0 + I_2(\alpha^2 + \beta^2),$$

$$m_{34} = -J_2(k_1 A' \alpha^2 + k_2 B' \beta^2),$$

$$m_{44} = K_2((k_1 A')^2 \alpha^2 + (k_2 B')^2 \beta^2), \quad m_{35} = J_0,$$

$$m_{55} = K_0$$

#### 4. Numerical results

In this study, various numerical examples are presented to verify the accuracy of the present HSDT in predicting the natural frequency of simply supported plates. The analytical solution of the present work is compared with those of other theories. FG plates made of two material combinations of metal and ceramic: Al/ZrO<sub>2</sub> and Al/Al<sub>2</sub>O<sub>3</sub> are considered. Their corresponding material properties are given in Table 1.

Table 1 Material properties of metal and ceramic

properties	Metal	Ceramic	
	Aluminum Al	Alumina Al <sub>2</sub> O <sub>3</sub>	Zirconia ZrO <sub>2</sub>
Young's modulus E(GPa)	70	380	200
Poisson's ratio $\nu$	0,3	0,3	0,3
Mass density $\rho(\text{kg/m}^3)$	2702	3800	5700

#### 4.1 Results of vibration analysis

##### 4.1.1 Example 1

On the one hand, numerical results for vibration analysis are presented (Table 2). A comparison of the results of the natural frequency obtained by the present theory for simply supported isotropic square plate is given. For convenience, the following non-dimensional natural frequencies and non-dimensional parameters of foundations are used

$$\hat{\omega} = \omega a^2 \sqrt{\rho h / D_0} \quad (30)$$

$$k_w = K_w a^4 / D_0 \quad (31)$$

$$k_s = K_s a^2 / D_0 \quad (32)$$

$$D_0 = Eh^3 / [12(1 - \nu^2)] \quad (33)$$

Table 2 presents the first eight no-dimensional natural frequencies. The obtained results are compared with 3-D exact solutions developed by Leissa (1973), Zhou *et al.* (2002), Nagino *et al.* (2008), a FSDT computed via DQM (differential quadrature element method) given by Liu and Liew (1999), and the HSDT theories studied by Shufrin and Eisenberger (2005), Hosseini-Hashemi *et al.* (2011), Akavci (2014) and Mantari (2015).

Inspection of the table 2, it can be seen that the values obtained by the present computation are very close with those given by 3-D exact and HSDTs theories with decreasing of thickness ratio 1000 to 5.

On the other hand, FG plates are studied (Al/Al<sub>2</sub>O<sub>3</sub>). The main aim of this computation is to verify the obtained results with 3-D exact solution performed by Jin *et al.* (2014) and Mantari (2015). For this purpose, the non-dimensional fundamental frequencies  $\bar{\omega}$  are given in Table 3, for different values of power law index  $p$  and thickness ratio. In this part, the relations of non-dimensional natural frequencies and parameters of elastic foundation were used (see Eqs. (34) to (40)). Again, an excellent agreement between the results is seen (for square and rectangular plates).

$$\bar{\omega} = \omega h \sqrt{\rho_m / E_m} \quad (34)$$

$$\beta = \omega h \sqrt{\rho_c / E_c} \quad (35)$$

$$\tilde{\omega} = (\omega a^2 / h) \sqrt{\rho_m / E_m} \quad (36)$$

$$\bar{\beta} = (\omega a^2 / h) \sqrt{\rho_c / E_c} \quad (37)$$

Table 2 Non-dimensional fundamental frequencies  $\hat{\omega} = \omega a^2 \sqrt{\rho h / D_0}$  for simply supported isotropic square plates

$a/h$	Theory	Mode ( $m,n$ )							
		(1,1)	(1,2)	(2,1)	(2,2)	(1,3)	(3,1)	(2,3)	(3,2)
1000	Leissa (1973)	19.7392	49.3480	49.3480	78.9568	98.6960	98.6960	128.3021	128.3021
	Zhou <i>et al.</i> (2002)	19.7115	49.3470	49.3470	78.9528	98.6911	98.6911	128.3048	128.3048
	Akavci (2014)	19.7391	49.3476	49.3476	78.9557	98.6943	98.6943	128.3020	128.3020
	Mantari (2015)	19.7405	49.3486	49.3486	78.9580	98.6967	98.6967	128.3049	128.3049
	Present	19.7391	49.3475	49.3475	78.9557	98.6943	98.6943	128.3019	128.3019
100	Liu and Liew (1999)	19.7319	49.3027	49.3027	78.8410	98.5150	98.5150	127.9993	127.9993
	Nagino <i>et al.</i> (2008)	19.7320	49.3050	49.3050	78.8460	98.5250	98.5250	128.0100	128.0100
	Akavci (2014)	19.7322	49.3045	49.3045	78.8456	98.5223	98.5223	128.0346	128.0346
	Mantari (2015)	19.7332	49.3086	49.3086	78.8550	98.5365	98.5365	128.0346	128.0346
	Present	19.7323	49.3049	49.3049	78.8467	98.5241	98.5241	128.0146	128.0146
10	Liu and Liew (1999)	19.0584	45.4478	45.4478	69.7167	84.9264	84.9264	106.5154	106.5154
	Nagino <i>et al.</i> (2008)	19.0653	45.4869	45.4869	69.8093	85.0646	85.0646	106.7350	106.7350
	Akavci (2014)	19.0850	45.5957	45.5957	70.0595	85.4315	85.4315	107.3040	107.3040
	Mantari (2015)	19.1190	45.7339	45.7339	70.3148	85.7622	85.7622	107.7376	107.7376
	Present	19.0914	45.6286	45.6286	70.1297	85.5289	85.5289	107.4422	107.4422
5	Shufrin and Eisenberger (2005)	17.4524	38.1884	38.1884	55.2539	65.3130	65.3130	78.9864	78.9864
	Hosseini-Hashemi <i>et al.</i> (2011)	17.4523	38.1883	38.1883	55.2543	65.3135	65.3135	78.9865	78.9865
	Akavci (2014)	17.5149	38.4722	38.4722	55.8358	66.1207	66.1207	80.1637	80.1637
	Mantari (2015)	17.5899	38.6582	38.6582	56.0674	66.3474	66.3474	80.3365	80.3365
	Present	17.5324	38.5275	38.5275	55.9053	66.1815	66.1815	80.1826	80.1826

Table 3 Comparison of non-dimensional fundamental frequencies  $\bar{\omega} = \omega h \sqrt{\rho_m / E_m}$  of Al/Al<sub>2</sub>O<sub>3</sub> FG plates

$b/a$	$a/h$	$P$	Theory		
			Jin <i>et al.</i> (2014)	Mantari (2015)	Present
1	10	0	0.1135	0.1137	0.1135
		1	0.0870	0.0883	0.0882
		2	0.0789	0.0806	0.0806
		5	0.0741	0.0756	0.0755
	5	0	0.4169	0.4183	0.4170
		1	0.3222	0.3271	0.3261
		2	0.2905	0.2965	0.2961
		5	0.2676	0.2726	0.2720
	2	0	1.8470	1.8543	1.8538
		1	1.4687	1.4803	1.4798
		2	1.3095	1.3224	1.3237
		5	1.1450	1.1565	1.1547
2	10	0	0.0719	0.0719	0.0718
		1	0.0550	0.0558	0.0560
		2	0.0499	0.0510	0.0513
		5	0.0471	0.0480	0.0482
	5	0	0.2713	0.2721	0.2713
		1	0.2088	0.2121	0.2123
		2	0.1888	0.1928	0.1938
		5	0.1754	0.1789	0.1794
	2	0	0.9570	1.3075	1.3055
		1	0.7937	1.0371	1.0381
		2	0.7149	0.9297	0.9335
		5	0.6168	0.8248	0.8253

$$k_w = K_w a^4 / \bar{D} \quad (38)$$

$$k_s = K_s a^2 / \bar{D} \quad (39)$$

with

$$\bar{D} = h^3 / 12(1 - \nu^2)[p(8 + 3p + p^2)E_m + 3(2 + p + p^2)E_c] / [(1 + p)(2 + p)(3 + p)] \quad (40)$$

The effect of power law index  $p$  on the non-dimensional fundamental frequency of moderately thick square plates ( $a/h=10$ ) for two FGMs (Al/ZrO<sub>2</sub> and Al/Al<sub>2</sub>O<sub>3</sub>) is displayed in Fig. 2. It can be seen that the non-dimensional frequency is higher when the Al<sub>2</sub>O<sub>3</sub> is employed in the top surface. Also from this figure, the eigenfrequency of a homogeneous material (Al/Al) is shown as reference value.

The Fig. 3 shows the effect of the aspect ratio  $a/b$  on the non-dimensional fundamental frequency for moderately thick plates ( $a/h=10$ ,  $p=1$ ) for the above two FGMs (Al/ZrO<sub>2</sub> and Al/Al<sub>2</sub>O<sub>3</sub>). Again we see that the non-dimensional frequency is higher when the material Al<sub>2</sub>O<sub>3</sub> is used in the top surface. However, the non-dimensional frequency is close to that of a homogenous material (Aluminum) for small values of the aspect ratio  $a/b$ .

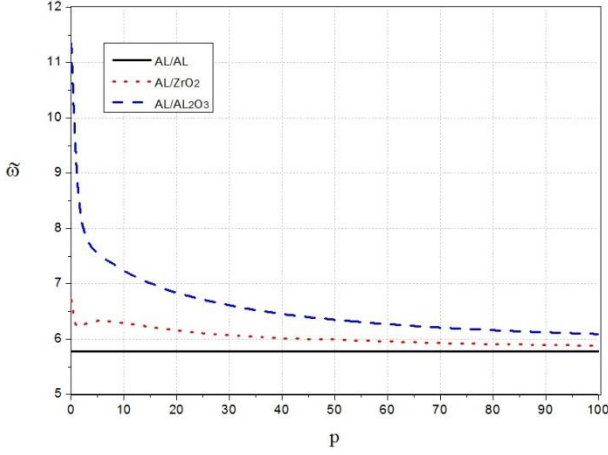


Fig. 2 Effect of power law index  $p$  on the non-dimensional fundamental frequency  $\tilde{\omega} = (\omega a^2 / h) \sqrt{\rho_m / E_m}$  of FG square plates ( $a/h=10$ )

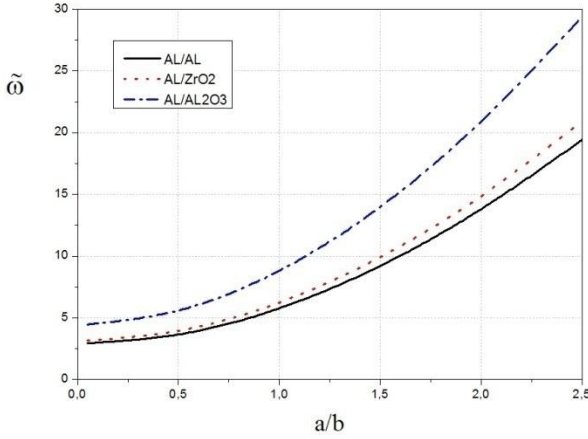


Fig. 3 Effect of the aspect ratio  $a/b$  on the non-dimensional fundamental frequency  $\tilde{\omega} = (\omega a^2 / h) \sqrt{\rho_m / E_m}$  of FG plates ( $a/h=10$ ,  $p=1$ )

The effect of the aspect ratio  $a/b$  on the non-dimensional frequency of FG plates resting on Winkler-Pasternak foundation is shown in Fig. 4. We can expect from this result that if the parameter  $k_s$  increases, the eigenfrequency increases, for a given aspect ratio  $a/b$  and parameter  $k_w$ .

Figs. 5 and 6 show the effect of elastic foundation parameters  $k_w$  and  $k_s$  respectively on the nondimensional frequency of FG square plates made of Al/Al<sub>2</sub>O<sub>3</sub>. It can be seen from this result that the curves, displayed on Fig. 5, present a linear trend for different values of  $k_w$ . However, the curves are greater slope to that obtained in Fig. 6. For this purpose, the influence of parameter  $k_s$  on the eigenfrequencies is greater compared to that of parameter  $k_w$ .

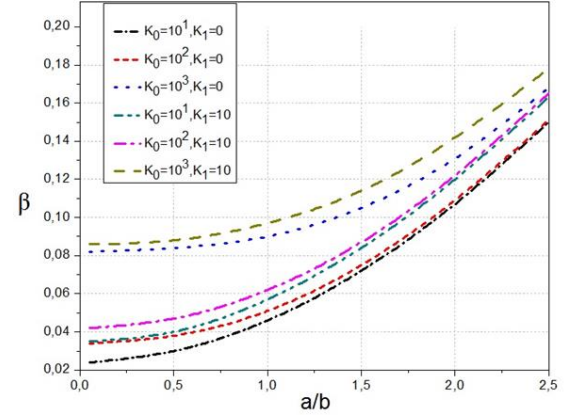


Fig. 4 Variation of non-dimensional fundamental frequency  $\beta = \omega h \sqrt{\rho_c / E_c}$  of Al/Al<sub>2</sub>O<sub>3</sub> FG rectangular plates resting on elastic foundation versus the aspect ratio ( $a/h=10$ ,  $p=1$ )

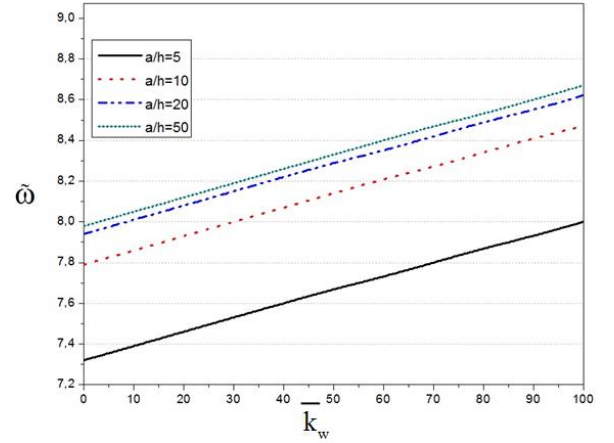


Fig. 5 Variation of non-dimensional fundamental frequency  $\tilde{\omega} = (\omega a^2 / h) \sqrt{\rho_m / E_m}$  of Al/Al<sub>2</sub>O<sub>3</sub> FG square plates resting on elastic foundation versus the parameter  $\bar{k}_w$  ( $k_s=10$ ,  $p=1$ )

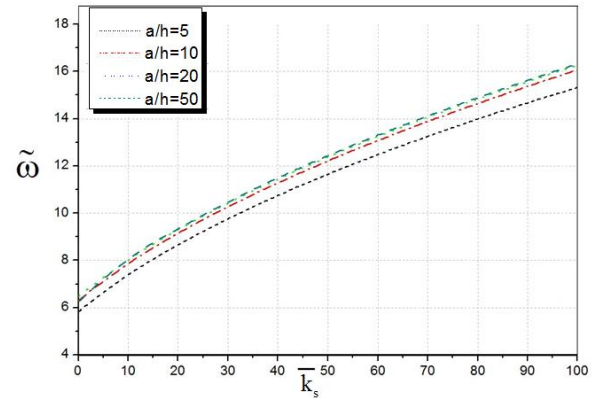


Fig. 6 Variation of non-dimensional fundamental frequency  $\tilde{\omega} = (\omega a^2 / h) \sqrt{\rho_m / E_m}$  of Al/Al<sub>2</sub>O<sub>3</sub> FG square plates resting on elastic foundation versus the parameter  $\bar{k}_s$  ( $k_w=10$ ,  $p=1$ )

## 5. Conclusions

In the present paper, a free vibration analysis of advanced composites plates resting on Winkler-Pasternak elastic foundation, using an efficient hybrid quasi-3D higher-order shear deformation theory was studied. This theory accounts for the thickness stretching and shear deformation effects without requiring an appropriate shear correction factor. It contains only five unknown functions and then five governing equations are only obtained. Moreover, the number of unknowns is reduced and is less than other theories found in the literature. The governing equations are deduced by utilizing Hamilton's principle. The equations of motion are solved analytically using the Navier's type solution. Furthermore, natural frequencies are obtained by solving the results of eigenvalue problems. The effects of power law index, thickness ratio and two-parameter elastic foundation on the natural frequencies are analyzed. The key conclusions that emerge from the numerical results can be summarized as follows:

- The accuracy of proposed hybrid quasi-3D higher-order theory is an excellent agreement compared with the FSDT and with other closed-form solutions published in the literature.
- For thick plates, the stretching effect is more pronounced and it needs to be taken account.
- The foundation stiffness affects the vibration of FGM plates.

## Acknowledgments

The authors would like to thank Cristina Maria e Silva de Sousa Lopes, from Faculty of Engineering University of Porto (FEUP), for his contribution in this work.

## References

- Abrate, S. (2008), "Functionally graded plates behave like homogeneous plates", *Compos. B Eng.*, **39**, 151-158.
- Abualnour, M., Houari, M.S.A., Tounsi, A., Adda Bedia, E.A. and Mahmoud, S.R. (2018), "A novel quasi-3D trigonometric plate theory for free vibration analysis of advanced composite plates", *Compos. Struct.*, **184**, 688-697.
- Ait Amar Meziane, M., Abdelaziz, H.H. and Tounsi, A. (2014), "An efficient and simple refined for buckling and free vibration of exponentially graded sandwich plates under various boundary conditions", *J. Sandw. Struct. Mater.*, **16**(3), 293-318.
- Ait Atmane H. and Tounsi, A. (2017), "Effect of thickness stretching and porosity on mechanical response of a functionally graded beams resting on elastic foundations", *Int. J. Mech. Mat.*, **13**(1), 71-84.
- Akavci, S.S. (2014), "An efficient shear deformation theory for free vibration of functionally graded thick rectangular plates on elastic foundation", *Compos. Struct.*, **108**, 667-676.
- Attia, A., Tounsi, A., Adda Bedia, E.A. and Mahmoud, S.R. (2015), "Free vibration analysis of functionally graded plates with temperature-dependent properties using various four variable refined plate theories", *Steel Compos. Struct.*, **18**(1), 187-212.
- Baferani, A.H., Saidi, A.R. and Jomehzadeh, E. (2011), "An exact solution for free vibration of thin functionally graded rectangular plates", *Proc. Inst. Mech. Eng. Part C*, **225**, 526-536.
- Bellifa, H., Benrahou, K.H., Hadji, L., Houari, M.S.A. and Tounsi, A. (2016), "Bending and free vibration analysis of functionally graded plates using a simple shear deformation theory and the concept the neutral surface position", *J. Brazil. Soc. Mech. Sci. Eng.*, **38** (1), 265-275.
- Bennoun, M., Houari, M.S.A. and Tounsi, A. (2016), "A novel five variable refined plate theory for vibration analysis of functionally graded sandwich plates", *Mech. Adv. Mater. Struct.*, **23**(4), 423-431.
- Bensaid, I., Cheikh, A., Mangouchi, A. and Kerboua, B. (2017), "Static deflection and dynamic behavior of higher-order hyperbolic shear deformable compositionally graded beams", *Adv. Mater. Res.*, **6**(1), 13-26.
- Bensattalah, T., Zidour, M., Tounsi, A. and Adda Bedia, E.A. (2016), "Investigation on thermal and chirality effects on vibration of single-walled carbon nanotubes embedded in a polymeric matrix using nonlocal elasticity theories", *Mech. Compos. Mater.*, **52**(4), 1-14.
- Bouazza, M., Amara, K., Zidour, M., Tounsi, A. and Adda Bedia, E.A. (2015), "Post-buckling analysis of nanobeams using trigonometric shear deformation theory", *Appl. Sci. Report.*, **10** (2), 112-121.
- Bouderba, B., Houari, M.S.A., Tounsi, A. and Mahmoud, S.R. (2016), "Thermal stability of Functionally graded sandwich plates using a simple shear deformation theory", *Struct. Eng. Mech.*, **58**(3), 397-422.
- Boukhari, A., Ait Atmane, H., Tounsi, A., Adda Bedia, E.A. and Mahmoud, S.R. (2016), "An efficient shear deformation theory for wave propagation of functionally graded material plates", *Struct. Eng. Mech.*, **57**(5), 837-859.
- Bousahla, A.A., Benyoucef, S., Tounsi, A. and Mahmoud, S.R. (2016), "On thermal stability of plates with functionally graded coefficient of thermal expansion", *Struct. Eng. Mech.*, **60**(2), 313-335.
- Chen, C.S., Chen, T.J. and Chien, R.D. (2006), "Nonlinear vibration of initially stressed functionally graded plates", *Thin-Walled Struct.*, **44**(8), 844-851.
- Feldman, E. and Aboudi, J. (1997), "Buckling analysis of functionally graded plates subjected to uniaxial loading", *Compos. Struct.*, **38**, 29-36.
- Hassaine Daouadji, T. and Hadji, L. (2015), "Analytical solution of nonlinear cylindrical bending for functionally graded plates", *Geomech. Eng.*, **9**(5), 631-644.
- Hosseini-Hashemi, Sh., Fadaee, M. and Rokni Damavandi Taher, H. (2011), "Exact solutions for free flexural vibration of Lévy-type rectangular thick plates via third-order shear deformation plate theory", *Appl. Math. Model.*, **35**, 708-727.
- Houari, M.S.A., Tounsi, A., Bessaim, A. and Mahmoud, S.R. (2016), "A new simple three-unknown sinusoidal shear deformation theory for functionally graded plates", *Steel Compos. Struct.*, **22**(2), 257-276.
- Javaheri, R. and Eslami, M. (2002), "Buckling of functionally graded plates under in-plane compressive loading", *J. Appl. Math. Mech.*, **82**, 277-283.
- Jha, D.K., Kant, T. and Singh, T.K. (2013), "Free vibration response of functionally graded thick plates with shear and normal deformations effects", *Compos. Struct.*, **96**, 799-823.
- Jin, G., Su, Z., Shi, S., Ye, T. and Gao, S. (2014), "Three-dimensional exact solution for the free vibration of arbitrarily thick functionally graded plates with general boundary conditions", *Compos. Struct.*, **108**, 565-577.
- Kar, V.R. and Panda, S.K. (2013), "Free Vibration Responses of Functionally Graded Spherical Shell Panels Using Finite Element Method", ASME 2013 Gas Turbine India Conference.
- Kar, V.R. and Panda, S.K. (2014), "Nonlinear free vibration of

- functionally graded doubly curved shear deformable panels using finite element method", *Vib. Control*, **22**(7), 1935-1945.
- Kar, V.R. and Panda, S.K. (2015a), "Nonlinear flexural vibration of shear deformable functionally graded spherical shell panel", *Steel Compos. Struct.*, **18**(3), 693-709.
- Kar, V.R. and Panda, S.K., (2015b), "Thermoelastic analysis of functionally graded doubly curved shell panels using nonlinear finite element method", *Compos. Struct.*, **129**, 202-212.
- Kar, V.R. and Panda, S.K. (2015c), "Free vibration responses of temperature dependent functionally graded curved panels under thermal environment ", *Latin Am. J. Solids Struct.*, **12**(11), 2006-2024.
- Kar, V.R. and Panda, S.K. (2015d), "Effect of temperature on stability behaviour of functionally graded spherical panel", *IOP Conference Series: Materials Science and Engineering*, **75**(1), 012014.
- Kar, V.R. and Panda, S.K. (2016a), "Geometrical nonlinear free vibration analysis of FGM spherical panel under nonlinear thermal loading with TD and TID properties", *J. Therm. Stresses*, **39**(8), 942-959.
- Kar, V.R. and Panda, S.K. (2016b), "Post-buckling behaviour of shear deformable functionally graded curved shell panel under edge compression", *Int. J. Mech. Sci.*, **115**, 318-324.
- Kar, V.R. and Panda, S.K. (2016c), "Nonlinear thermomechanical deformation behaviour of P-FGM shallow spherical shell panel", *Chinese J. Aeronaut.*, **29**(1), 173-183.
- Kar, V.R. and Panda, S.K., (2016d), "Nonlinear thermomechanical behavior of functionally graded material cylindrical/hyperbolic/elliptical shell panel with temperature-dependent and temperature-independent properties", *J. Pressure Vessel Technol.*, **138**(6), 061202-061202-13.
- Kar, V.R. and Panda, S.K. (2017a), "Postbuckling analysis of shear deformable FG shallow spherical shell panel under nonuniform thermal environment", *J. Therm. Stresses*, **40**(1), 25-39.
- Kar, V.R. and Panda, S.K. (2017b), "Large-amplitude vibration of functionally graded doubly-curved panels under heat conduction", *AIAA J.*, **55**(12), 4376-4386.
- Kar, V.R., Mahapatra, T.R. and Panda, S.K. (2017), "Effect of different temperature load on thermal postbuckling behaviour of functionally graded shallow curved shell panels", *Compos. Struct.*, **160**(15), 1236-1247.
- Kar, V.R. (2015a), "Nonlinear flexural vibration of shear deformable functionally graded spherical shell panel", *Steel Compos. Struct.*, **18**(3), 693-709.
- Kar, V.R. (2015b), "Large deformation bending analysis of functionally graded spherical shell using FEM", *Struct. Eng. Mech.*, **53**(4), 661-679.
- Karami, B. and Janghorban, M. (2016), "Effect of magnetic field on the wave propagation in nanoplates based on strain gradient theory with one parameter and two-variable refined plate theory", *Modern Phys. Lett. B*, **30** (36).
- Karami, B., Janghorban, M. and Li, L. (2018), "On guided wave propagation in fully clamped porous functionally graded nanoplates", *Acta Astronautica*, **143**, 380-390.
- Karami, B., Shahsavari, D. and Janghorban, M. (2017), "Wave propagation analysis in functionally graded (FG) nanoplates under in-plane magnetic field based on nonlocal strain gradient theory and four variable refined plate theory", *Mech. Adv. Mater. Struct.*, 1-11.
- Karami, B., Shahsavari, D. and Janghorban, M. (2018), "Wave dispersion of mounted graphene with initial stress". *Thin-Wall. Struct.*, **122**, 102-111.
- Khdeir, A.A. and Reddy, J.N. (1999), "Free vibrations of laminated composite plates using second-order shear deformation theory". *Compos. Struct.*, **71**, 617-626.
- Koizumi, M. (1993), "The concept of FGM", *Ceram. Trans. Func. Grad. Mater.*, **34**, 3-10.
- Koizumi, M. (1997), "FGM activities in Japan", *Compos. Part. B Eng.*, **28** (1-2), 1-4.
- Leissa, A.W. (1973), "The free vibration of rectangular plates", *J. Sound Vib.*, **31**(3), 257-293.
- Liu, F.L. and Liew, K.M. (1999), "Analysis of vibrating thick rectangular plates with mixed boundary constraints using differential quadrature element method", *J. Sound Vib.*, **225** (5), 915-934.
- Mahapatra, T.R., Kar, V.R., Panda, S.K. and Mehar, K. (2017), "Nonlinear thermoelastic deflection of temperature-dependent FGM curved shallow shell under nonlinear thermal loading", *J. Therm. Stresses*, **40**(9), 1184-1199.
- Mahdavian, M. (2009), "Buckling analysis of simply-supported functionally graded rectangular plates under non-uniform in-plane compressive loading", *J. Solid. Mech.*, **1**, 213-225.
- Mahi, A., Adda Bedia, E.A. and Tounsi, A. (2015), "A new hyperbolic shear deformation theory for bending and free vibration analysis of isotropic functionally graded sandwich and laminated composite plates", *Appl. Math. Model.*, **39**(9), 2489-2508.
- Mantari, J.L. and Granados, E.V. (2015), "Free vibration of single and sandwich laminated composite plates by using a simplified FSDT", *Compos. Struct.*, **132**, 952-959.
- Mantari, J.L. (2015), "A refined theory with stretching effect for the dynamic analysis of advanced composites on elastic foundation", *Mech. Mater.*, **86**, 31-43.
- Mantari, J.L. (2015), "Refined and generalized hybrid type quasi-3D shear deformation theory for the bending analysis of functionally graded shells", *Compos. B. Eng.*, **83**, 142-152.
- Mantari, J.L., Oktem, A.S. and Soares, C.G. (2012), "A new Higher order shear deformation theory for sandwich and composite laminated plates", *Compos. B. Eng.*, **43**(3), 1489-1499.
- Meftah, A., Bakora, A., Zaoui, F.Z., Tounsi, A. and Adda Bedia, E., (2017), "A non-polynomial four variable refined plate theory for free vibration of functionally graded thick rectangular plates on elastic foundations", *Steel Compos. Struct.*, **23**(3), 317-330.
- Meksi, A., Benyoucef, S., Houari, M.S.A. and Tounsi, A., (2015), "A simple shear deformation theory based on neutral surface position for functionally graded plates resting on Pasternak elastic foundations", *Struct. Eng. Mech.*, **53**(6), 1215-1240.
- Miyamoto, Y., Kaysser, W.A., Rabin, B.H. and Ford, R.G. (1999), *Functionally graded materials: design, processing and applications*, London: Kluwer Academic publishers.
- Mohammedi, M., Saidi, A.R. and Jomehzadeh, E., (2010), "Levy solution for buckling analysis of functionally graded rectangular plates", *Appl. Compos. Mater.*, **17**, 81-93.
- Nagino, H., Mikami, T. and Mizusawa, T. (2008), "Three-dimensional free vibration analysis of isotropic rectangular plates using the B-spline Ritz method", *J. Sound Vib.*, **317**, 329-353.
- Nami, M.R., Janghorban, M. and Damadam, M. (2015), "Thermal buckling analysis of functionally graded rectangular nanoplates based on nonlocal third-order shear deformation theory", *Aerosp. Sci. Technol.*, **41**, 7-15.
- Neves, A.M.A., Ferreira, A.J.M., Carrera, E., Cinefra, M., Jorge, R.M.N. and Soares, C.M. (2012), "Buckling analysis of sandwich plates with functionally graded skins using a new quasi-3D hyperbolic sine shear deformation theory and collocation with radial basis functions", *J. Appl. Math. Mech.*, **92**(9), 749-766.
- Neves, A.M.A., Ferreira, A.J.M., Carrera, E., Cinefra, M., Jorge, R.M.N., Mota Soares, C.M., et al. (2017), "Influence of zig-zag and warping effects on buckling of functionally graded sandwich plates according to sinusoidal shear deformation

- theories", *Mech. Adv. Mater. Struct.*, **24**(5), 360-376.
- Neves, A.M.A., Ferreira, A.J.M., Carrera, E., Cinefra, M., Roque, C.M.C., Jorge, R.M.N., et al. (2012), "A quasi-3D hyperbolic shear deformation theory for the static and free vibration analysis of functionally graded plates", *Compos. Struct.*, **94**(5), 1814-1825.
- Neves, A.M.A., Ferreira, A.J.M., Carrera, E., Cinefra, M., Roque, C.M.C., Jorge, R.M.N., et al. (2012), "A quasi-3D sinusoidal shear deformation theory for the static and free vibration analysis of functionally graded plates", *Compos. B. Eng.*, **43**(2), 711-725.
- Nguyen, K., Thai, H.T. and Vo, T. (2015), "A refined higher-order shear deformation theory for bending, vibration and buckling analysis of functionally graded sandwich plates", *Steel Compos. Struct.*, **18** (1), 91-120.
- Reddy, J.N. (2000), "Analysis of functionally graded plates", *Int. J. Numer. Method. Eng.*, **47**, 663-684.
- Reddy, J.N. (2002), "Energy principles and variational methods in applied mechanics", *John Wiley & Sons*.
- Saidi, A.R. and Sahraee, S. (2006), "Axisymmetric solutions of functionally graded circular and annular plates using second-order shear deformation plate theory", ESDA2006-95699, *Proceedings of the 8th Biennial ASME Conference on Engineering Systems Design and Analysis*, Torino, Italy.
- Shahrjerdi, A. and Mustapha, F. (2011), "Second Order Shear Deformation Theory (SSDT) for Free Vibration Analysis on a Functionally Graded Quadrangle Plate", *Recent Advances in Vibrations Analysis*, (Ed., Natalie Baddour).
- Shahsavari, D., Karami, B. and Mansouri, S. (2018), "Shear buckling of single layer graphene sheets in hygrothermal environment resting on elastic foundation based on different nonlocal strain gradient theories", *Eur. J. Mech. A-Solid*, **67**, 200-214.
- Shahsavari, D., Shahsavari, M., Li, L. and Karami, B. (2018), "A novel quasi-3D hyperbolic theory for free vibration of FG plates with porosities resting on Winkler/Pasternak/Kerr foundation", *Aerosp. Sci. Technol.*, **72**, 134-149.
- Shimpi, R. and Patel, H. (2006), "Free vibrations of plate using two variable refined plate theory", *J. Sound Vib.*, **296**, 979-999.
- Shufrin, I. and Eisenberger, M., (2005), "Stability and vibration of shear deformable plates – first order and higher order analyses", *Int. J. Solids Struct.*, **42**, 1225-1251.
- Sobhy, M., (2013), "Buckling and free vibration of exponentially graded sandwich plates resting on elastic foundations under various boundary conditions", *Compos. Struct.*, **99**, 76-87.
- Xu, T.F. and Xing, Y.F. (2016), "Closed-form solutions for free vibration of rectangular FGM thin plates resting on elastic foundation", *Acta Mech. Sin.*, **32**(6), 1088-1103.
- Yaghoobi, H. and Yaghoobi, P. (2013), "Buckling analysis of sandwich plates with FGM face sheets resting on elastic foundation with various boundary conditions: an analytical approach", *Meccanica*, **48**(8), 2019-2039.
- Zhang, D.G. and Zhou, Y.H. (2008), "A theoretical analysis of FGM thin plates based on physical neutral surface", *Comput. Mater. Sci.*, **44**, 716-720.
- Zhou, D., Cheung, Y.K., Au, F.T.K. and Lo, S.H. (2002), "Three-dimensional vibration analysis of thick rectangular plates using Chebyshev polynomial and Ritz method", *Int. J. Solids Struct.*, **39**, 6339-6353.